Sea level rise, spatially uneven and temporally unsteady: Why the U.S. East Coast, the global tide gauge record, and the global altimeter data show different trends

Tal Ezer[1]

Received 10 September 2013; revised 30 September 2013; accepted 4 October 2013; published 17 October 2013.

[1] Impacts of ocean dynamics on spatial and temporal variations in sea level rise (SLR) along the U.S. East Coast are characterized by empirical mode decomposition analysis and compared with global SLR. The findings show a striking latitudinal SLR pattern. Sea level acceleration consistent with a weakening Gulf Stream is maximum just north of Cape Hatteras and decreasing northward, while SLR driven by multidecadal variations, possibly from climatic variations in subpolar regions, is maximum in the north and decreasing southward. The combined impact of sea level acceleration and multidecadal variations explains why the global mean SLR obtained from ~20 years of altimeter data is about twice the century-long global SLR obtained from tide gauge data. The sea level difference between Bermuda and the U.S. coast is highly correlated with the transport of the Atlantic Overturning Circulation, a result with implications for detecting past and future climatic changes using tide gauge data. **Citation:** Ezer, T. (2013), Sea level rise, spatially uneven and temporally unsteady: Why the U.S. East Coast, the global tide gauge record, and the global altimeter data show different trends, *Geophys. Res. Lett.*, *40*, 5439–5444, doi:10.1002/2013GL057952.

1. Introduction

[2] The mid-Atlantic region along the East Coast of the United States has been identified as a "hot spot" of accelerated sea level rise (SLR) since sea level acceleration (i.e., an increase with time of SLR rate) there is much larger than global acceleration [*Boon*, 2012; *Ezer and Corlett*, 2012; *Sallenger et al*., 2012; *Kopp*, 2013]. As a result of this fast regional SLR, low-lying coastal communities in the mid-Atlantic region have seen a significant increase in the frequency of flooding in recent years [*Atkinson et al*., 2013]. In addition to large land subsidence around the Chesapeake Bay area [*Boon et al*., 2010; *Kopp*, 2013], SLR acceleration in the mid-Atlantic has been found to be highly correlated with recent offshore shift and weakening in the Gulf Stream (GS) just north of Cape Hatteras (CH) as seen in altimeter data [*Ezer et al*., 2013, hereinafter E13] (see also Figure S5 in the supporting information). The latter finding is consistent with dynamic sea level changes seen in ocean models [*Ezer*, 1999, 2001; *Levermann et al*., 2005; *Yin et al*., 2009] and expected weakening in the Atlantic Meridional Overturning Circulation (AMOC) under warmer climate conditions [*Hakkinen and Rhines*, 2004; *Sallenger et al*., 2012; *McCarthy et al*., 2012; *Srokosz et al*., 2012]. Though there have been some signs of weakening AMOC since 2004 and weakening GS in the mid-Atlantic since 2004 (E13), the long-term downward trend in the strength of the GS may not be statistically significant so far [*Rossby et al*., 2005, also personal communication, 2013].

[3] The existence of SLR acceleration in the global ocean is even more difficult to assess than the regional acceleration, so published results do not always agree with each other [*Church and White*, 2011; *Houston and Dean*, 2011; *Baart et al*., 2012; *Dean and Houston*, 2013]. One of the hotly debated issues addressed here is the discrepancy between the mean global SLR obtained from ~130 years of global tide gauge data (~1.5 mm yr^{-1}) and that obtained from ~20 years of altimeter data (~3.2 mm yr^{-1}). Is this discrepancy an indication of global SLR acceleration, difference in coverage, instrumental errors, or unresolved long-term cycles? (e.g., the 60 year cycle) [*Chambers et al*., 2012]. Comparisons between tide gauges and altimeter data are often inconclusive about the exact reason for this discrepancy [*Dean and Houston*, 2013]. To address the above problems, the empirical mode decomposition/Hilbert-Huang transformation (EMD/HHT) method [*Huang et al*., 1998; *Wu and Huang*, 2009] was used, following the methodology of *Ezer and Corlett* [2012]. Nonparametric methods such as the EMD and the Gaussian Process (GP) decomposition [*Kopp*, 2013] may have some advantages over standard least squares fitting methods commonly used in sea level studies (see the supporting information).

[4] This study has two main goals: (1) to extend the EMD sea level analysis, previously applied only to the Chesapeake Bay [*Ezer and Corlett*, 2012] and the Mid-Atlantic Bight (E13), to most of the East Coast of the United States, so that connections between spatial patterns in SLR and ocean dynamics can be established; and (2) to study how decadal and multidecadal variations affect SLR and explain the discrepancy between global SLR of tide gauge data and altimeter data.

2. Data and Analysis Methods

[5] Monthly mean sea level records from 11 tide gauge stations with over 60 years of high-quality data (see Table S1) were obtained from the Permanent Service for Mean Sea Level (www.psmsl.org) [*Woodworth and Player*, 2003]. The data include 10 stations along the U.S.

[1]Center for Coastal Physical Oceanography, Old Dominion University, Norfolk, Virginia, USA.

Corresponding author: T. Ezer, Center for Coastal Physical Oceanography, Old Dominion University, 4111 Monarch Way, Norfolk, VA 23508, USA. (tezer@odu.edu)

0094-8276/13/10.1002/2013GL057952

Figure 1. Map of the study area indicating the location of the 11 tide gauge stations used and the location of the cable across the Florida Strait which measures the transport of the Florida Current (red line). Schematics of the Florida Current and the Gulf Stream mean flow are shown.

East Coast, from Boston, MA, to Key West, FL, and one station offshore, in the North Atlantic Ocean at Bermuda (Figure 1). Altimeter and tide gauge global sea level data are obtained from the Commonwealth Scientific and Industrial Research Organization (www.cmar.csiro.au/sealevel/) [*Church and White*, 2011]. Florida Current (FC) transport data are from cable measurements across the Florida Strait at 27°N (NOAA/AOML; www.aoml.noaa.gov/phod/floridacurrent/); the data include the periods 1982–1998 and 2000–2012. Semidaily AMOC transport at 26.5°N for 2004–2012 was obtained from the RAPID project (www.rapid.ac.uk/rapidmoc) [*McCarthy et al*., 2012].

[6] The analysis method of all time series is based on the EMD (see supporting information), whereas each record is decomposed into a finite number of intrinsic oscillatory modes and a residual "trend" $r(t)$. The frequency in each mode is time dependent, but here modes are grouped in a way that each time series is represented by $\boldsymbol{\eta}(t) = \mathrm{HF}(t) + \mathrm{DO}(t) + \mathrm{MD}(t) + r(t)$, where HF is the sum of the high-frequency modes with average periods $T < 5$ years, DO is the sum of decadal oscillation modes with periods 5 years $< T <$ 15 years, and MD is the sum of multidecadal variations with periods $T > 15$ years. A *multidecadal trend* is defined as $\mathrm{MD}(t) + r(t)$. Land movement (mostly postglacial rebound) is not directly addressed by the EMD but is assumed to have a linear trend, so comparisons between local and global linear SLR trends will tell us about land movement. On the other hand, nonlinear EMD-derived acceleration, $r(t)$, will indicate processes other than land motion (likely ocean dynamics). Figures S1 and S2 show examples of the EMD analysis for the records of sea level in New York and in the global mean sea level, respectively; both records show a positive SLR acceleration. Mode 7, for example, resembles the 60 year cycle discussed by *Chambers et al*. [2012], showing that the local and global sea level records are in phase since ~1920. The low-frequency modes in New York (modes 5–9 in Figure S1) show upward recent trends, which suggest multiple contributions to the recent SLR acceleration. Experiments with ensemble EMD calculations [*Wu and Huang*, 2009] demonstrate that the trends are very robust and insensitive to even high levels of white noise (Figure S3).

3. Results

3.1. Spatial Variations in SLR Trends and Sea Level Acceleration

[7] The linear trends in SLR are shown in Figure 2a, and the mean rates are shown in Figure 3a and listed in Table S1. The large SLR rates in the mid-Atlantic, from Atlantic City to Norfolk, are due to large land subsidence around the Chesapeake Bay [*Boon et al*., 2010; *Kopp*, 2013]; the lowest SLR rate at Wilmington (2.01 mm yr^{-1}) and the highest SLR rate at Norfolk (4.66 mm yr^{-1}) are from close geographical locations but represent different geological settings (the postglacial rebound and the Chesapeake Impact Crater increase land subsidence, especially in the lower Chesapeake Bay [*Boon et al*., 2010]). The SLR trends obtained from the EMD analysis (Figure 2b) are clearly nonlinear and show almost universal positive SLR acceleration (Figure 3b). The spatial pattern of acceleration is much more striking than linear trends (Figure 3a) and is likely the result of ocean dynamics, since long-term geological processes are quite linear and thus were eliminated in Figure 3b. The statistically significant positive acceleration north of Cape Hatteras (CH) is

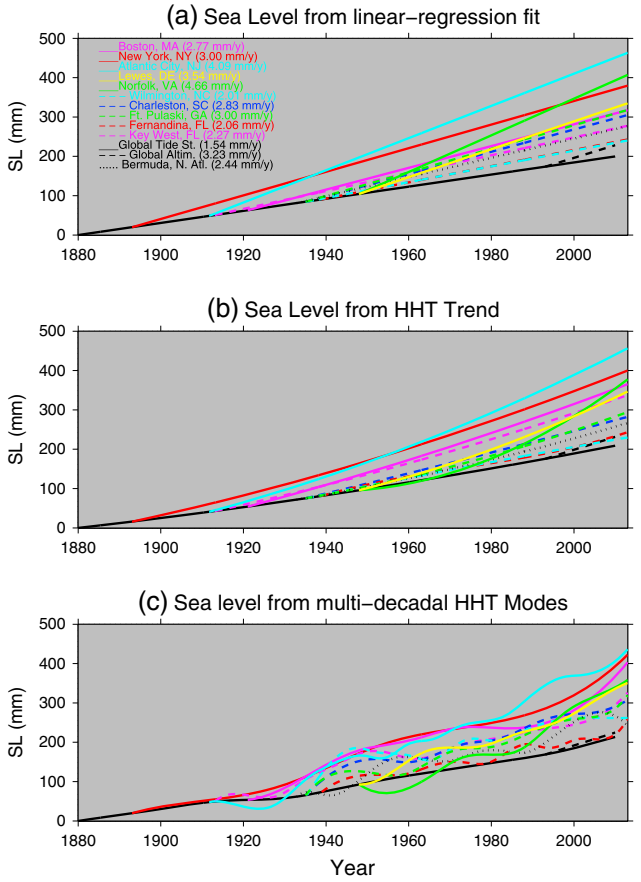

Figure 2. Comparisons between the global sea level obtained from tide gauges (black solid line starting in 1880), from altimeter data (dashed black line starting in 1993), and from local sea level data. Solid/dashed color lines are for coastal tide gauges located north/south of Cape Hatteras on the U.S. coast, and the dotted black line is from Bermuda in the Atlantic Ocean (see Figure 1). Each local record is shifted to match the global mean sea level at the beginning of the record. (a) Linear regression fit lines (the mean sea level rise of each record is indicated). (b) Nonlinear long-term trend obtained from the residual of the EMD analysis. (c) Multidecadal trend of the EMD analysis.

in agreement with the SLR acceleration calculated by quadratic least squares methods [*Boon*, 2012; *Sallenger et al.*, 2012] or GP decomposition [*Kopp*, 2013]. However, the above previous studies show significant SLR acceleration mostly after 1970, while the EMD method removes multidecadal variations from the trend and calculates mean acceleration [i.e., the average of the second derivative of $r(t)$; see equations (S4a) and (S4b)] over entire records. Thus, the EMD calculations give more credibility to the assessment that the "hot spot of accelerated SLR" is real. The global tide gauge data show small positive acceleration, but the global altimeter data show negative acceleration, though the altimeter record length, ~20 years, is too short to make any conclusions from this result. Based on the bootstrap ensemble simulations of *Ezer and Corlett* [2012], the 95% confidence interval around the mean acceleration calculated by the EMD is estimated to be about ±0.01 mm yr^{-2} (see supporting information for details). Therefore, statistically significant positive SLR acceleration is found in Boston, New York, Atlantic City, Lewes, Norfolk, Pulaski, and Bermuda. The spatial pattern of the acceleration in Figure 3b is quite striking, showing a decrease in the impact of the GS as one moves north from CH along the coast, extending the SLR-GS correlation pattern found by E13. Figures 3a and 3b also show the impact of record length on the analysis by comparing the results of the full records with results obtained from the past 60 years ("diamond" markers; see also Figure S4). While the impact of record length on mean linear SLR is relatively small, it is affecting sea level acceleration more profoundly, indicating that SLR rates are in fact changing over time. In particular, the distinction between large positive acceleration north of CH and insignificantly small acceleration south of CH is enhanced over the past 60 years, providing further confirmation to the hot spot of accelerated SLR findings of *Sallenger et al.* [2012]. The significant increase in acceleration over the past 60 years in Boston and New York reflects the impact of multidecadal variations, as discussed in the next section.

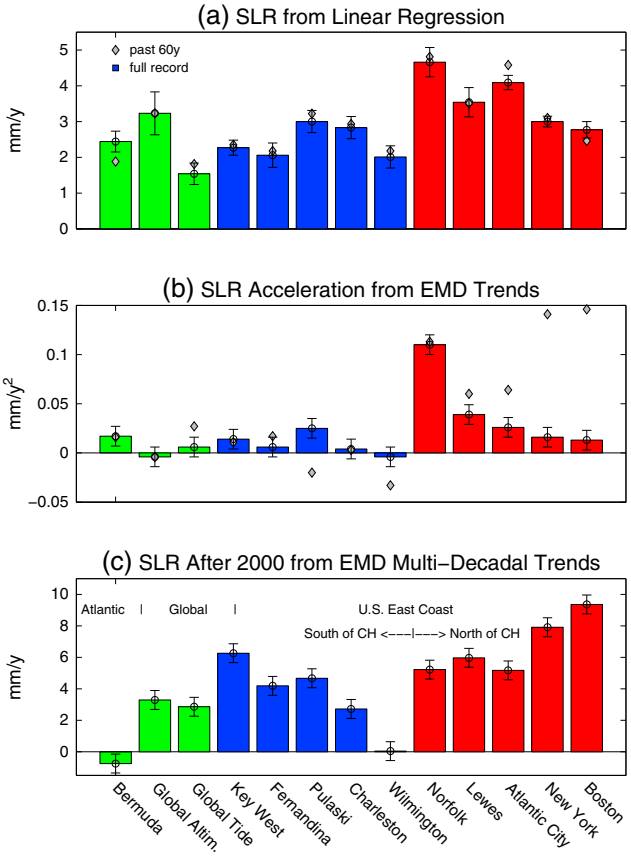

Figure 3. (a) SLR rates obtained from linear regression (see Figure 2a). (b) Average SLR acceleration obtained from the trend of the EMD (see Figure 2b). (c) Sea level rise rates after 2000 obtained from the multidecadal trend of the EMD (see Figure 2c). Red/blue bars are for locations north/south of Cape Hatteras, and green bars are for the global data and the Atlantic Ocean data (Bermuda). The diamond markers in Figures 3a and 3b are for calculations over the past 60 years (all records with about the same length except the shorter altimeter record that remains unchanged; see also Figure S4). The supporting information explains the estimated error bars (95% confidence intervals).

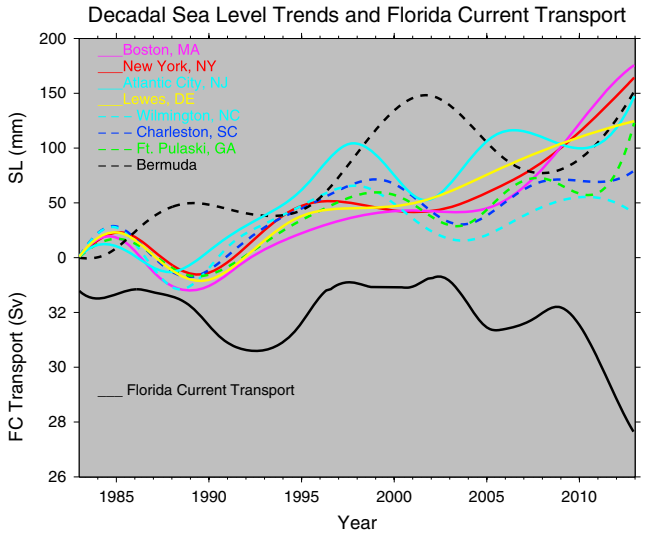

Figure 4. Decadal to multidecadal variations in sea level (top lines) and the Florida Current transport (black solid line on the bottom). Note that the sea level variations on the U.S. coast (color lines) are often in opposite phase to that in Bermuda (dashed black line).

3.2. Multidecadal Variations and Global SLR From Tide Gauges and Altimeter Data

[8] Both the linear trend (Figure 3a) and the acceleration (Figure 3b) show large discrepancy between the global SLR rates obtained from tide gauges and those obtained from altimeter data (even an opposite sign of acceleration). To examine if multidecadal variations are responsible for this discrepancy, the multidecadal sea level trend MD*(t)* + *r(t)* is shown in Figure 2c, and the mean SLR rate after 2000 is shown in Figure 3c. The multidecadal trends show time-dependent SLR rates, thus complicating any calculations based on linear regression. The most interesting result in Figure 3c is that now, the recent SLR rate of the global ocean calculated from tide gauge data (2.86 ± 0.6 mm yr^{-1}) is almost the same as that calculated from altimeter data (3.29 ± 0.6 mm yr^{-1}), i.e., only 15% difference between the two measurements compared with 110% difference in the long-term linear trends (1.54 versus 3.23 mm yr^{-1}, respectively). The results suggest that recent high SLR rates in the global ocean are likely due to the combination of long-term acceleration, *r(t)*, and multidecadal variations, MD*(t)*. The spatial pattern of recent coastal SLR shown in Figure 3c is in sharp contrast with the SLR acceleration pattern in Figure 3b. The highest MD influence on SLR is in New York and Boston and reducing influence toward CH, suggesting that the source of the multidecadal variations may be climatic changes in subpolar regions [*Hakkinen and Rhines*, 2004] which impact the Labrador Sea outflow [*Rossby et al*., 2005]. Some increase in recent SLR due to multidecadal variations is also seen southward from CH, suggesting potential impact from variations in the subtropical gyre. The closeness of the GS to the coast south of CH seems to limit shifts in the GS position and changes in its strength compared with locations north of CH (Figure S5), explaining the small sea level changes there, as shown in Figure 3. The location closest to the GS separation point, Wilmington, shows the smallest value for all three SLR indicators, namely, the mean SLR rate, the sea level acceleration, and the impact of multidecadal variations (Figure 3).

3.3. The Relation Between Sea Level, the Gulf Stream, and the AMOC

[9] Sea level records (for clarity, eight records are shown) are compared with the Florida Current (FC) transport in Figure 4, focusing on time scales of decadal and longer, i.e., the combination of DO*(t)* + MD*(t)* + *r(t)* from the EMD analysis. The sea level of all the stations along the U.S. coast shows similar patterns of decadal oscillations with minima around 1989 and 2004 and maxima around 1985 and 1999; sea level in Bermuda seems to be in an opposite phase to the coastal stations until about 2007 with distinct maxima around 1989 and 2002. During periods of large differences in sea level between Bermuda and the U.S. coast, such as 1987–1991 and 1999–2004, the FC transport is large, while in years following a weak FC, such as 1992–1994, 2005–2007, and 2011-2012, there is no significant difference in sea level between Bermuda and the U.S. coast. Therefore, it does seem that the sea level difference between the coastal U.S. and the Atlantic (i.e., Bermuda) can detect variations in the GS, as previously shown in ocean models [*Ezer*, 1999, 2001]. Over the past 5 years of data, the pattern has changed with the GS transport declining and sea level rising (similar to the results of E13 who used a shorter GS record from altimeter data). This recent GS slowdown may relate to climate-related weakening of the AMOC, as suggested by *Yin et al*. [2009], *Sallenger et al*. [2012], and others. Observations of the AMOC transport across 26.5°N are available since 2004 [*McCarthy et al*., 2012]; this record is relatively short, but does it correlate with sea level data? Figure 5 shows a comparison between the EMD modes of the AMOC and those of the sea level difference between Bermuda and Atlantic City after adding a 2 month lag (sea level lags behind AMOC, though the reason of which needs further research). The monthly records of sea level difference and AMOC are significantly correlated ($R = 0.27$ at 95% confidence level), but much higher correlations are found for some modes, in particular, in mode 4 (~3 year period), with $R = 0.81$, and the long-term trends in the AMOC and the sea level (mode 6) are almost identical ($R > 0.99$), with downward trends after 2008. A combination of the low-frequency EMD modes demonstrates the possibility to infer the AMOC transport from sea level (Figure 5, right bottom). Note the significant decline from 2009 to 2010 of the AMOC and the sea level difference that is captured by mode 4.

4. Summary and Conclusions

[10] The study suggests explanations for recent findings of accelerated SLR (hot spot) along the U.S. East Coast north of CH [*Boon*, 2012; *Ezer and Corlett*, 2012; *Sallenger et al*., 2012; *Kopp*, 2013] and the impact of climate-related changes in the AMOC [*Hakkinen and Rhines*, 2004; *McCarthy et al*., 2012; *Srokosz et al*., 2012] and its upper branch, the GS, on SLR. By expanding the results of E13 from the mid-Atlanic region to most of the U.S. East Coast, the results provided further evidence for the role of ocean dynamics on uneven SLR patterns and the role of multidecadal variations on recent SLR.

[11] Two outstanding questions were addressed: (1) how changes in ocean dynamics affect the spatial pattern of

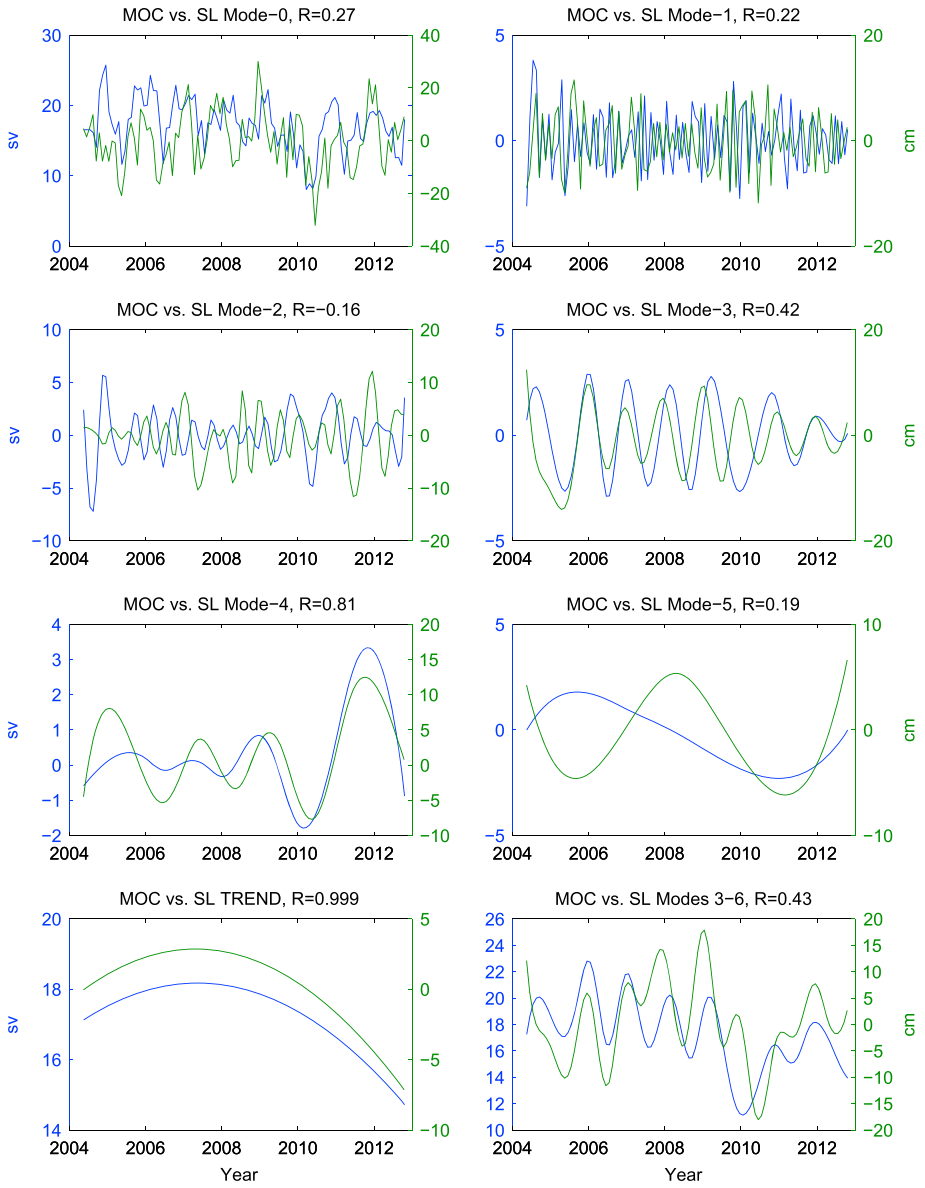

Figure 5. EMD analysis of the Meridional Overturning Circulation (MOC) [*McCarthy et al.*, 2012] time series (blue lines; units in sverdrups on the left) and sea level (SL) difference between Bermuda and Atlantic City (green lines; units in centimeters on the right); *R* is the correlation coefficient between MOC and SL. Mode 0 is the original monthly data, and modes 1–5 are oscillating modes with decreasing frequency. (bottom left) Residual trend (mode 6). (bottom right) Sum of modes 3–6.

SLR along the U.S. East Coast and (2) how decadal and multidecadal variations affect local and global SLR. The EMD analysis shows a clearer spatial pattern of SLR (Figure 3b) than standard least squares curve fitting methods do (Figure 3a), since long-term trends are separated from decadal, multidecadal, and interannual variations. The fact that the long-term SLR acceleration is maximum just north of CH and reduces northward confirms the finding of E13 of maximum GS-SLR correlations in the southern portion of the Mid-Atlantic Bight, where recent slowdown of the GS seemed to increase SLR rates. South of CH, the SLR acceleration is comparable to the (small) global and Atlantic values. A possible reason why the hot spot does not extend southward beyond CH is that south of CH, the GS is flowing closer to the coastline and has smaller variability and cross-stream gradient compared with the GS downstream of the separation point at CH (Figure S5). Another interesting finding is that when multidecadal variations are added to the long-term sea level trend, SLR rates over the last decade or so (Figure 3c) are maximum at high latitudes and decreasing southward toward CH. This result signals that the source of the multidecadal variations in sea level in high latitudes may be coming from climatic variations in subpolar regions [*Hakkinen and Rhines*, 2004]. Decadal and multidecadal variations in sea level are coherent along the U.S. East Coast but are in opposite phase to sea level in Bermuda. Therefore, it was shown here that the difference in sea level between Bermuda and the U.S. coast (i.e., across the GS and its northern recirculation gyre) may be a proxy for changes in the GS and the AMOC. Since sea level is more easily measured and has longer record than AMOC observations, this result may have important implications for studying past and future climatic changes.

[12] The EMD analysis also provides an explanation for the discrepancy in mean SLR (and opposite acceleration

sign) obtained from ~20 years of global altimeter data and ~130 years of global tide gauge data. When multidecadal variations are added to the long-term trend, the recent global SLR rates of the past decade for altimeter and tide gauge data are almost the same. The results suggest that global SLR is accelerating in recent years but that this acceleration is a combination of long-term trends and multidecadal variations.

[13] **Acknowledgments.** Old Dominion University's Climate Change and Sea Level Rise Initiative (CCSLRI) as well as the Center for Coastal Physical Oceanography (CCPO) provided partial support for this study. T. Ezer was partly supported by grants from NOAA's Climate Programs.

[14] The Editor thanks Robert Kopp and an anonymous reviewer for their assistance in evaluating this paper.

References

Atkinson, L. P., T. Ezer, and E. Smith (2013), Sea level rise and flooding risk in Virginia, *Sea Grant Law Policy J.*, *5*(2), 3–14.

Baart, F., M. van Koningsveld, and M. J. F. Stive (2012), Trends in sea-level trend analysis, *J. Coastal Res.*, *28*(2), 311–325.

Boon, J. D. (2012), Evidence of sea level acceleration at U.S. and Canadian tide stations, Atlantic coast, North America, *J. Coastal Res.*, *28*(6), 1437–1445, doi:10.2112/JCOASTRES-D-12-00102.1.

Boon, J. D., J. M. Brubaker, and D. R. Forrest (2010), *Chesapeake Bay Land Subsidence and Sea Level Change: An Evaluation of Past and Present Trends and Future Outlook*, Applied Marine Science and Ocean Engineering Report No. 425, Va. Inst. of Mar. Sci., Gloucester Point, Va.

Chambers, D. P., M. A. Merrifield, and R. S. Nerem (2012), Is there a 60-year oscillation in global mean sea level?, *Geophys. Res. Lett.*, *39*, L18607, doi:10.1029/2012GL052885.

Church, J. A., and N. J. White (2011), Sea-level rise from the late 19th to the early 21st century, *Surv. Geophys.*, *32*, 585–602, doi:10.1007/s10712-011-9119-1.

Dean, R. G., and J. R. Houston (2013), Recent sea level trends and accelerations: Comparison of tide gauge and satellite results, *Coastal Eng.*, *75*, 4–9, doi:10.1016/j.coastaleng.01.001.

Ezer, T. (1999), Decadal variabilities of the upper layers of the subtropical North Atlantic: An ocean model study, *J. Phys. Oceanogr.*, *29*(12), 3111–3124.

Ezer, T. (2001), Can long-term variability in the Gulf Stream transport be inferred from sea level?, *Geophys. Res. Lett.*, *28*(6), 1031–1034.

Ezer, T., and W. B. Corlett (2012), Is sea level rise accelerating in the Chesapeake Bay? A demonstration of a novel new approach for analyzing sea level data, *Geophys. Res. Lett.*, *39*, L19605, doi:10.1029/2012GL053435.

Ezer, T., L. P. Atkinson, W. B. Corlett, and J. L. Blanco (2013), Gulf Stream's induced sea level rise and variability along the U.S. mid-Atlantic coast, *J. Geophys. Res. Oceans*, *118*, 685–697, doi:10.1002/jgrc.20091.

Hakkinen, S., and P. B. Rhines (2004), Decline of subpolar North Atlantic Circulation during the 1990s, *Science*, *304*, 555–559.

Houston, J. R., and R. G. Dean (2011), Sea-level acceleration based on U.S. tide gauges and extensions of previous global-gauge analyses, *J. Coastal Res.*, *27*(3), 409–417.

Huang, N. E., Z. Shen, S. R. Long, M. C. Wu, E. H. Shih, Q. Zheng, C. C. Tung, and H. H. Liu (1998), The empirical mode decomposition and the Hilbert spectrum for non stationary time series analysis, *Proc. R. Soc. London, Ser. A*, *454*, 903–995.

Kopp, R. E. (2013), Does the mid-Atlantic United States sea-level acceleration hot spot reflect ocean dynamic variability?, *Geophys. Res. Lett.*, *40*, 3981–3985, doi:10.1002/grl.50781.

Levermann, A., A. Griesel, M. Hofmann, M. Montoya, and S. Rahmstorf (2005), Dynamic sea level changes following changes in the thermohaline circulation, *Clim. Dyn.*, *24*(4), 347–354.

McCarthy, G., E. Frejka-Williams, W. E. Johns, M. O. Baringer, C. S. Meinen, H. L. Bryden, D. Rayner, A. Duchez, C. Roberts, and S. A. Cunningham (2012), Observed interannual variability of the Atlantic Meridional Overturning Circulation at 26.5°N, *Geophys. Res. Lett.*, *39*, L19609, doi:10.1029/2012GL052933.

Rossby, T., C. N. Flagg, and K. Donohue (2005), Interannual variations in upper-ocean transport by the Gulf Stream and adjacent waters between New Jersey and Bermuda, *J. Mar. Res.*, *63*(1), 203–226.

Sallenger, A. H., K. S. Doran, and P. Howd (2012), Hotspot of accelerated sea-level rise on the Atlantic coast of North America, *Nat. Clim. Change*, *2*, 884–888, doi:10.1038/NCILMATE1597.

Srokosz, M., M. Baringer, H. Bryden, S. Cunningham, T. Delworth, S. Lozier, J. Marotzke, and R. Sutton (2012), Past, present, and future changes in the Atlantic meridional overturning circulation, *Bull. Am. Meteorol. Soc.*, *1*, 1663–1676, doi:10.1175/BAMS-D-11-00151.

Woodworth, P. L., and R. Player (2003), The permanent service for mean sea level: An update to the 21st century, *J. Coastal Res.*, *19*(2), 287–295.

Wu, Z., and N. E. Huang (2009), Ensemble empirical mode decomposition: A noise-assisted data analysis method, *Adv. Adapt. Data Anal.*, *1*(01), 1–41.

Yin, J., M. E. Schlesinger, and R. J. Stouffer (2009), Model projections of rapid sea-level rise on the northeast coast of the United States, *Nat. Geosci.*, *2*, 262–266, doi:10.1038/NGEO462.

Sea level rise, spatially uneven and temporally unsteady: why the U. S. east coast, the global tide gauge record and the global altimeter data show different trends

(Supplementary material)

Tal Ezer

Center for Coastal Physical Oceanography, Old Dominion University, Norfolk, Virginia, USA.
Email: tezer@odu.edu; Web: http://www.ccpo.odu.edu/Facstaff/faculty/tezer/ezer.html

Contents:

1. The EMD/HHT analysis method

The analysis method of all time series is based on the Empirical Mode Decomposition and Hilbert-Huang Transformation [EMD/HHT; *Huang et al*., 1998; *Wu et al*., 2007; *Huang and Wu*, 2008; *Wu and Huang*, 2009], as implemented for sea level rise (SLR) studies by *Ezer and Corlett* [2012a,b]. *Ezer et al*. [2013] used the EMD analysis to correlate variations in the Gulf Stream with variations in coastal sea level, suggesting that recent weakening in the Gulf Stream may be responsible for increasing SLR rates along the Chesapeake Bay and the mid-Atlantic coast. This SLR acceleration may be the main cause for recent increase of flooding in the area [*Sweet et al*, 2009; *Atkinson et al*., 2013; *Boesch et al*., 2013; *Mitchell et al*., 2012]. The method has been recently used for example, to analyze various climate records [*Pietrafesa et al*., 2013] and to study internal waves in the ocean [*Ezer et al*., 2011].

EMD/HHT is a non-parametric analysis for non-stationary time series whereas a record is decomposed into a finite number, N, of intrinsic oscillatory modes $c_i(t)$ and a residual "trend" $r(t)$, so that an EMD of a sea level record from location M (or from global mean record) would be represented by

$$\eta^M(t) = \sum_{i=1}^{N} c_i{}^M(t) + r^M(t) \quad . \tag{s1}$$

The definition of the trend in the EMD calculation is "a time-dependent function with at most one extremum representing either a mean trend or a constant" [*Wu et al*., 2007]. However, the method is "non-parametric", so no specific functional shape is imposed on the trend (in contrast to least square regression analysis). The number of modes is not predetermined and depends on the variability in the record (in our case N is typically in the range 8 to10). The frequency in each mode is time dependent but it is useful to group the modes in the following way,

$$\eta^M(t) = HF^M(t) + DO^M(t) + MD^M(t) + r^M(t) \quad , \tag{s2}$$

where HF is the sum of the high-frequency modes with average periods T < 5yr (seasonal and interannual variations), DO is the sum of decadal oscillation modes with periods 5yr < T < 15yr, and MD is the sum of multi-decadal variations with periods T > 15yr. Note that *multi-decadal variations* refer to $MD(t)$, while *multi-decadal trends* refer to $MD(t)+r(t)$, as defined by *Wu et al.* [2007]. The approach here is somewhat similar to the Gaussian Process (GP) decomposition approach of *Kopp* [2013], though it is more general and does not have any parameters to chose. On the other hand, the GP provides a better statistical framework than the EMD (see supplementary material in *Kopp* for review of various analysis methods). The purpose of (s2) is to look at coherent features between the local and global sea level. In comparison, linear regression analysis represents the time series as

$$\eta^M(t) = A^M + B^M t \quad . \tag{s3}$$

The mean SLR rate and SLR acceleration in the linear regression are B and zero, respectively, while in the EMD analysis they are defined as

$$SLR^{EMD} = \frac{1}{T}\int_{t=0}^{T}\frac{dr}{dt}dt \;;\; ACC^{EMD} = \frac{1}{T}\int_{t=0}^{T}\frac{d^2r}{dt^2}dt \quad , \qquad \text{(s4a, s4b)}$$

where T is the record length in years. *Ezer and Corlett* [2012a] showed that SLR^{EMD} is almost identical to B. ACC^{EMD} will indicate deceleration/linear trend/acceleration in SLR for negative/zero/positive values.

The calculations above for all sea level records (see locations in Fig. 1) are summarized in supplementary Table S1, and two examples of the EMD analysis are shown in supplementary Fig. S1 and Fig. S2, for two of the longest records, sea level in New York and the global mean sea level record [*Church and White*, 2011], respectively. In Fig. S1 and Fig. S2, *HF* (high-frequency, seasonal and interannual variability) is represented by modes 1-4, *DO* by modes 5-6, *MD* by modes 7-8 and *r* by mode 9. Features common to the local (Fig. S1) and global (Fig. S2) records are the positive SLR acceleration seen in the trend (mode 9) and the similar pattern of mode 7 which resembles the 60-year cycle discussed by *Chambers et al*. [2012] and others. An interesting result is that several low-frequency modes are now in an upward trend that can contribute to recent increase in SLR in New York (mode 5 is up after 2005, mode 6 after 2000, modes 7-8 after ~1990, and mode 9 since 1900). This result demonstrates the complexity of understanding SLR forcing, whereas several simultaneous processes may affect SLR rates. Therefore, using a simple linear regression to calculate trends may not tell the whole story.

Since the frequency of each oscillating EMD mode is not constant, one of the shortcomings of the method is the potential of aliasing when one physical process may affect several modes, or when noise in one mode affect the frequency of another mode [*Huang et al*., 1998; *Huang and Wu*, 2008]. One way to test the robustness of the analysis is using Ensemble EMD (EEMD) where the results are not based on a singular EMD calculation, but on the mean of a series of calculations, each one with an added random white noise (*Wu and Huang*, 2009). Therefore, ten EEMD calculations with ten different noise levels are shown in Fig. 3 for the New York record; each calculation represents an ensemble of 50 members, with a total of 500 EMD calculations. These results show that both, the multi-decadal variability (Fig. 3Sa) and the trend (Fig. 3Sb) are extremely robust with no apparent aliasing even when noise as large as the signal itself is added. The conclusion from this test is that uncertainties in high frequency modes have little effect on the calculated long-term trends.

Another common problem with analysis of sea level data is that record lengths differ (Table S1), which can influence the SLR rates if the rate is not linear [*Baart et al*., 2012]. To test if the spatial pattern seen in Fig. 3 is affected by the record length, the SLR linear rates and accelerations are calculated using only 60 years of tide station data (1952-2012); 60 years is considered a record length with a reasonable confidence level for linear regressions [*Douglas*, 2001; *Zervas*, 2009]. The pattern of linear SLR has not changed much (Fig. S4a versus Fig. 3a), and the distinct positive acceleration north of Cape Hatteras remains statistically significant (Fig. S4b versus Fig. 3b). South of Cape Hatteras acceleration is small and thus more affected by record length (e.g., at Ft. Pulaski acceleration changed sign), so longer records are needed for statistical significance. The acceleration in Boston and New York over the past 60 years is larger than that obtained from the full record. That result is consistent with the fact that these two stations are most affected by multi-decadal oscillations (Fig. 3c), so in analyses of shorter records multi-decadal oscillations affect acceleration. Positive acceleration in the global tide record over the past 60 years (~0.03 ± 0.01 mm y^{-2}) is statistically significant and larger than that

calculated from ~130 years of data, which is consistent with the increase in SLR over the past 20 years seen in altimeter data.

2. Estimated errors

In Table S1, the mean SLR is from standard linear regression (i.e., B in Eq. s3), the mean acceleration is from the EMD trend (Eq. s4b), and SLR after 2000 is from the EMD multi-decadal trend (i.e., as in Eq. s4a, but from $(d/dt)(MD+r)$, where T is the period from 2000 to the end of the record). Errors of linear regression are based on *Zevas* [2009], whereas for a measured period of T years, the 95% confidence interval (CI) of the mean SLR obtained from linear regression is estimated to be $CI=395.5T^{-1.6431}$. The confidence interval for the EMD analysis is more complex, so it is based on the statistics of bootstrap simulations [*Mudelsee*, 2010] as described by *Ezer and Corlett* [2012a]. The bootstrap simulations can also be used for calculating future sea level projections [*Ezer and Corlett* [2012b]. Experiments with hundreds of bootstrap simulations (randomly re-sampling the anomalies in the data itself for each simulation) show that CI ~0.5 mm y^{-1} for each monthly SLR value, CI ~0.15 mm y^{-1} for a 10-year mean SLR and CI ~0.05 mm y^{-1} for a 60-year mean SLR. Note also that to achieve SLR accuracy of ~±0.5 mm y^{-1} at 95% statistical confidence using linear regression it is advised to have at least 60 years of data [*Douglas*, 2001; *Zervas*, 2009; *Boon et al*., 2010], while the error bars achieved by the EMD and the bootstrap simulations are much smaller, and less dependent on record length because of the ability of the EMD to separate the trend from other oscillating cycles.

Error bars in the mean SLR acceleration calculated from the EMD trend is similarly estimated from bootstrap simulations to be CI ~0.01 mm y^{-2}; CI was found to be quite insensitive to record length when using more than 500 simulations. To estimate the recent SLR of the multi-decadal records (Fig. 3c and Supplemental Table S1) it is assume that the CI of each of the low frequency modes are about the same, CI ~0.2 mm y^{-1}, so the total error of adding 3 modes is CI ~0.6 mm y^{-1}. The global mean monthly records have about tenth of the variability of individual records, so the bootstrap simulations result in CI of the EMD trends that are much smaller than errors associated with the fact that global records are averages of many individual records. Therefore, the CIs of the global records are estimated from published studies [*Woodworth and Player*, 2003; *Church and White*, 2011; others], instead of from the EMD errors of individual records. It should be emphasized here that the estimated error bars of the EMD mean rates show the robustness of the EMD analysis, given the observed variability; these estimated errors are not necessarily comparable with errors derived from least-square or other methods. Therefore, there is larger confidence in comparisons between different records within EMD results (Figs. 3b, 3c), than comparisons between EMD results and linear regression results (Fig. 3a). *Ezer and Corlett* [2012a] compared SLR mean rates and acceleration obtained by the EMD method with results obtained by other methods [*Boon et al*., 2010; *Boon*, 2012; *Sallenger et al*., 2012], and the latest results from *Kopp* [2013] and *Yin and Goddard* [2013] are also comparable to the EMD results. While an acceleration rate at particular individual record may slightly differ for each method, the relative change between one station to another, and in particular the spatial pattern of acceleration, are very consistent across different methods, and it is essential for studies of SLR not to relay on a single methods.

3. Gulf Stream variations north and south of Cape Hatteras

It is clear from the analysis of *Ezer et al.* (2013) and Fig. 3 here that variations in the Gulf Stream (GS) location and strength north and south of Cape Hatteras are very different and thus the impact on SLR is different. To demonstrate this, Fig. S5 shows altimeter-derived cross sections of sea level across the GS. Between September 2000 and September 2011 a large offshore shift in the GS north wall north of Cape Hatteras is accommodated by an increase in the southward flowing slope current (sea level slope opposite to GS slope) and a sea level rise of ~12cm at the mouth of the Chesapeake Bay. However, south of Cape Hatteras, where the GS flows closer to the coast, there is no apparent consistent interannual shift in the GS position over the same period (may be a small inshore shift) and no consistent sea level change at the coast except large weekly variations associated with meso-scale variability.

Supplementary References

Atkinson, L. P., T. Ezer and E. Smith, (2013), Sea level rise and flooding risk in Virginia, *Sea Grant Law and Policy Journal, Vol. 5, No. 2*, 3-14.

Baart, F., M. van Koningsveld and M. J. F. Stive, (2012), Trends in sea-level trend analysis, *J. Coast. Res.*, *28(2),* 311-325.

Boesch, D.F., L.P. Atkinson, W.C. Boicourt, J.D. Boon, D.R. Cahoon, R.A. Dalrymple, T. Ezer, B.P. Horton, Z.P. Johnson, R.E. Kopp, M. Li, R.H. Moss, A. Parris, C.K. Sommerfield, (2013), Updating Maryland's Sea-level Rise Projections, *Special Report of the Scientific and Technical Working Group to the Maryland Climate Change Commission*, 22 pp. University of Maryland Center for Environmental Science, Cambridge, MD.

Boon, J. D. (2012) Evidence of sea level acceleration at U.S. and Canadian tide stations, Atlantic coast, North America, *J. Coast. Res., 28*(6), 1437 – 1445, doi:10.2112/JCOASTRES-D-12-00102.1.

Boon, J. D., J. M. Brubaker and D. R. Forrest (2010), Chesapeake Bay land subsidence and sea level change, in *App. Mar. Sci. and Ocean Eng*., *Report No. 425,* Virginia Institute of Marine Science, Gloucester Point, VA.

Chambers, D. P., M. A. Merrifield, and R. S. Nerem (2012), Is there a 60-year oscillation in global mean sea level?, *Geophys. Res. Lett., 39*, L18607, doi:10.1029/2012GL052885.

Church, J. A. and N. J. White (2011), Sea-level rise from the late 19th to the early 21st century, Surv. *Geophys*., *32,* 585–602, doi:10.1007/s10712-011-9119-1.

Douglas, B. C. (2001), Sea level change in the era of the recording tide gauge, in Sea Level Rise: History and Consequences, Int. Geophys. Ser., vol.75, edited by B. C. Douglas, M. S. Kearney, and S. P. Leatherman, chap.3, pp.37–64, Elsevier, NewYork.

Ezer, T., W. D. Heyman, C. Houser and B. Kjerfve (2011), Modeling and observations of high-frequency flow variability and internal waves at a Caribbean reef spawning aggregation site. *Ocean Dynamics*, 61(5), 581-598, doi:10.1007/s10236-010-0367-2.

Ezer, T. and W. B. Corlett (2012a), Is sea level rise accelerating in the Chesapeake Bay? A demonstration of a novel new approach for analyzing sea level data, *Geophys. Res. Lett*., *39*, L19605, doi:10.1029/2012GL053435.

Ezer, T. and W. B. Corlett (2012b), Analysis of relative sea level variations and trends in the Chesapeake Bay: Is there evidence for acceleration in sea level rise? Proc. Oceans'12 MTS/IEEE, Paper# 120509-002, IEEE Xplore, 1-5, doi: 10.1109/OCEANS.2012.6404794.

Ezer, T., L. P. Atkinson, W. C. Corlett and J. L. Blanco (2013), Gulf Stream's induced sea level rise and variability along the U.S. mid-Atlantic coast. *J. Geophys. Res*. 118(2), 685–697, doi:10.1002/jgrc.20091.

Huang, N. E., Z. Shen S. R. Long,M. C. Wu, E. H. Shih, Q. Zheng, C. C. Tung, H. H. Liu (1998), The Empirical Mode Decomposition and the Hilbert spectrum for non stationary time series analysis, *Proc. Roy. Soc. Lond., 454,* 903–995.

Huang, N. E. and Z. Wu (2008), A review on Hilbert-Huang transform: the method and its applications on geophysical studies, *Rev. Geophys*.,*46*, RG2006, doi:10.1029/2007RG000228.

Kopp, R. E. (2013), Does the mid-Atlantic United States sea level acceleration hot spot reflect ocean dynamics variability?. *Geophys. Res. Lett*., doi:10.1002/grl.50781.

Mitchell, M., C. Hershner, J. Herman, D. Schatt, E. Eggington, and S. Stiles (2013), *Recurrent flooding study for Tidewater Virginia*, Report SJR 76, 2012, Virginia Institute of Marine Science, Gloucester Point, VA, pp. 141.

Mudelsee, M. (2010), *Climate Time Series Analysis: Classical Statistical and Bootstrap Methods*, Springer, 474 pp., doi:10.1007/978-90-481-9482-7.

Pietrafesa, L. J., D. A. Dickey, P. T. Gayes, T. Yan, J. M. Epps, M. Hagan, S. Bao and M. Peng (2013), On atmospheric-oceanic-land temperature variability and trends. *Intern. J. Geosci*., 4, 417-443.

Sweet, W., C. Zervas and S. Gill (2009), Elevated east coast sea level anomaly: June-July 2009, *NOAA Tech. Rep. No. NOS CO-OPS 051*, NOAA National Ocean Service, Silver Spring, MD, 40pp.

Wu, Z. and Huang, N. E. (2009), Ensemble empirical mode decomposition: a noise-assisted data analysis method. *Advances in Adaptive Data Analysis*, *1*(01), 1-41.

Wu, Z., N. E. Huang, S. R. Long, and C.-K. Peng (2007), On the trend, detrending and variability of nonlinear and non-stationary time series. *Proc Nat. Acad. Sci., USA, 104*, 14889-14894.

Woodworth, P. L. and R. Player (2003), The Permanent Service for Mean Sea Level: An Update to the 21stCentury, J. Coastal Res., 19(2), 287-295.

Zervas, C. (2009), Sea level variations of the United States 1854-2006. NOAA Tech. Rep. NOS CO-OPS 053, 78pp, NOAA/National Ocean Service, Silver Spring, MD.

Yin, J. and P. Goddard (2013), Oceanic control of sea level rise patterns along the east coast of the United States. *Geophys. Res. Lett*., under revision.

Supplementary Table S1. Monthly sea level data used in this study. Column A is from linear regression (corresponds to Fig. 3a), column B is from the trend plus multi-decadal modes, *r*+*MD*, averaged for the period after 2000 (Fig. 3c) and column C is from the time-mean slope of *r* over the entire record (Fig. 3b).

Station	Latitude	Longitude	Period	**A** mean SLR (mm/y)	**B** SLR after 2000 (mm/y)	**C** SLR Accel (mm/y^2)
Boston, MA	42.35°N	71.05°W	1921-2012	2.77±0.23	9.36±0.6	0.013±0.01
New York, NY	40.70°N	74.01°W	1893-2012	3.00±0.15	7.91±0.6	0.016±0.01
Atlantic City, NJ	39.36°N	74.42°W	1911-2012	4.09±0.20	5.17±0.6	0.026±0.01
Lewes, DE	38.78°N	75.12°W	1947-2012	3.54±0.41	5.97±0.6	0.039±0.01
Norfolk, VA	36.95°N	76.33°W	1948-2012	4.66±0.41	5.22±0.6	0.110±0.01
Wilmington, NC	34.23°N	77.95°W	1935-2012	2.01±0.31	0.04±0.6	-0.004±0.01
Charleston, SC	32.78°N	79.93°W	1935-2012	2.83±0.31	2.72±0.6	0.004±0.01
Ft. Pulaski, GA	32.03°N	80.90°W	1935-2012	3.00±0.31	4.67±0.6	0.025±0.01
Fernandina, FL	30.67°N	81.47°W	1939-2012	2.06±0.34	4.19±0.6	0.006±0.01
Key West, FL	24.56°N	81.81°W	1913-2012	2.27±0.21	6.26±0.6	0.014±0.01
Bermuda	32.37°N	64.70°W	1932-2012	2.44±0.29	-0.75±0.6	0.017±0.01
Global Tide	-	-	1880-2009	1.54±0.3	2.86±0.6	0.006±0.01
Global Altimeter	-	-	1993-2009	3.23±0.6	3.29±0.6	-0.004±0.01

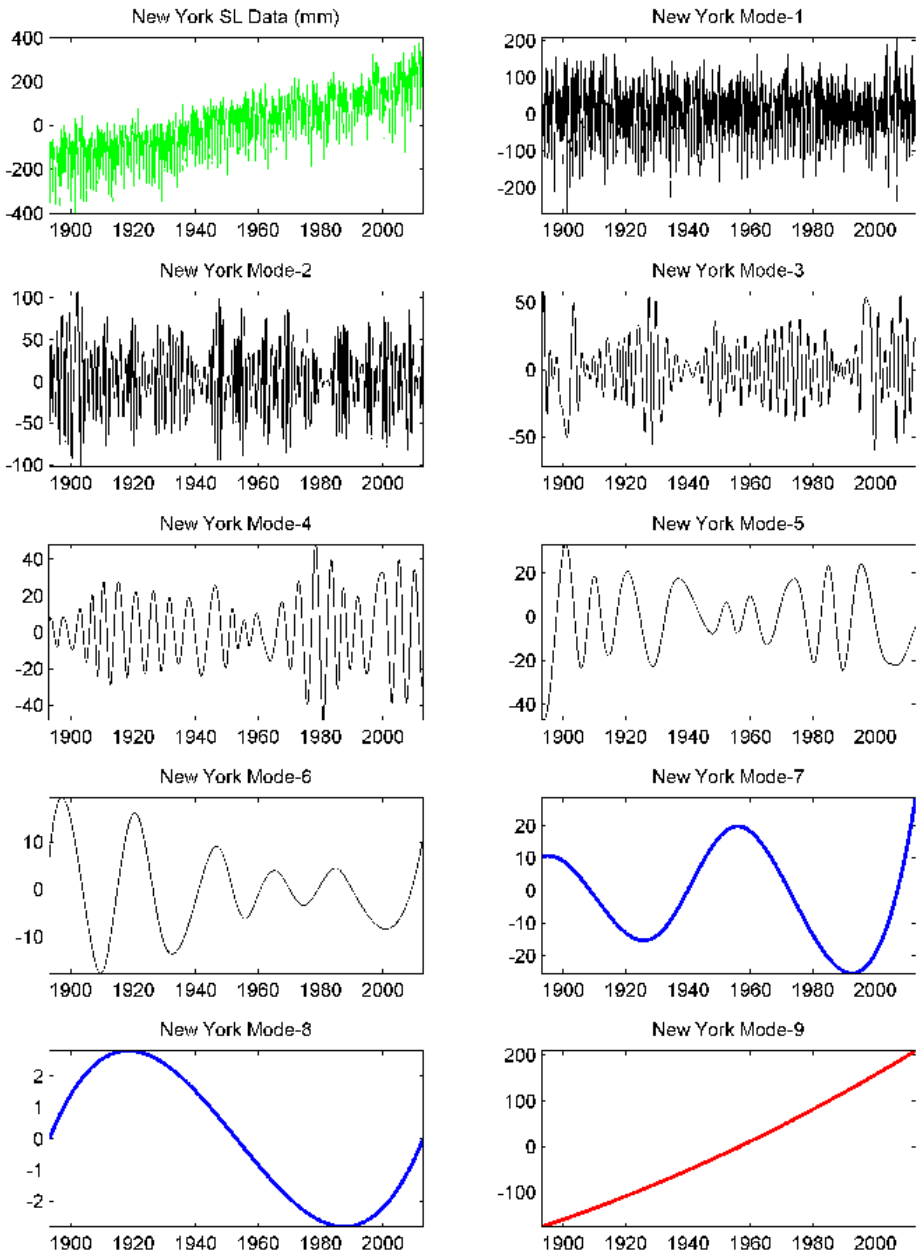

Figure S1. The EMD/HHT analysis for the New York sea level data. The original monthly data (green) is decomposed into intra-seasonal to decadal oscillating modes (black), multi-decadal modes (blue) and long-term residual trend (red).

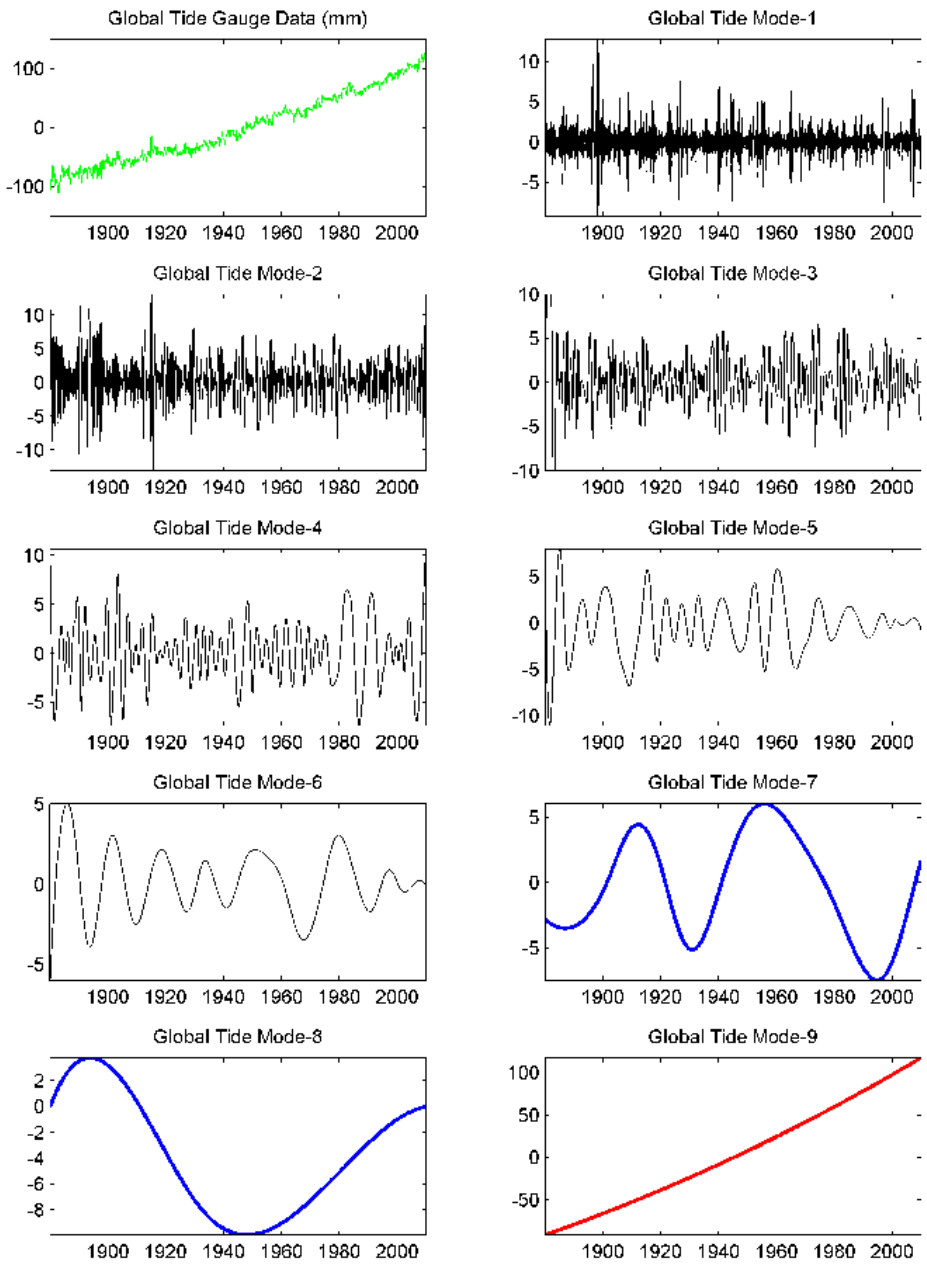

Figure S2. Same EMD/HHT as Fig. S2, but for the global mean sea level.

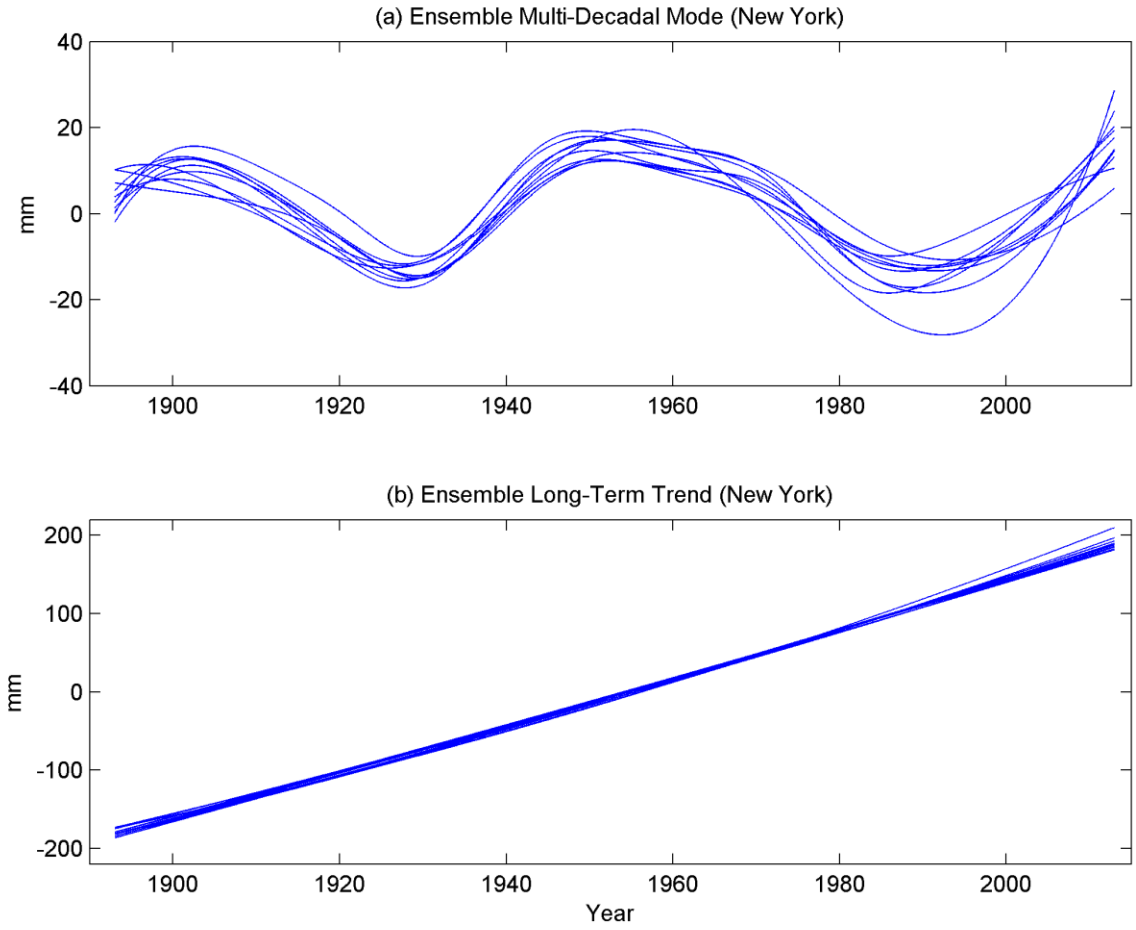

Figure S3. Test of the robustness of (a) multi-decadal modes *MD(t)* and (b) long-term trend *r(t)*, using EEMD for New York sea level record. Each line represents an average of an ensemble of 50 members with different white noise level added to the original monthly data. The standard deviation of the random noise is 10%, 20%,…100% of the standard deviation of the actual data.

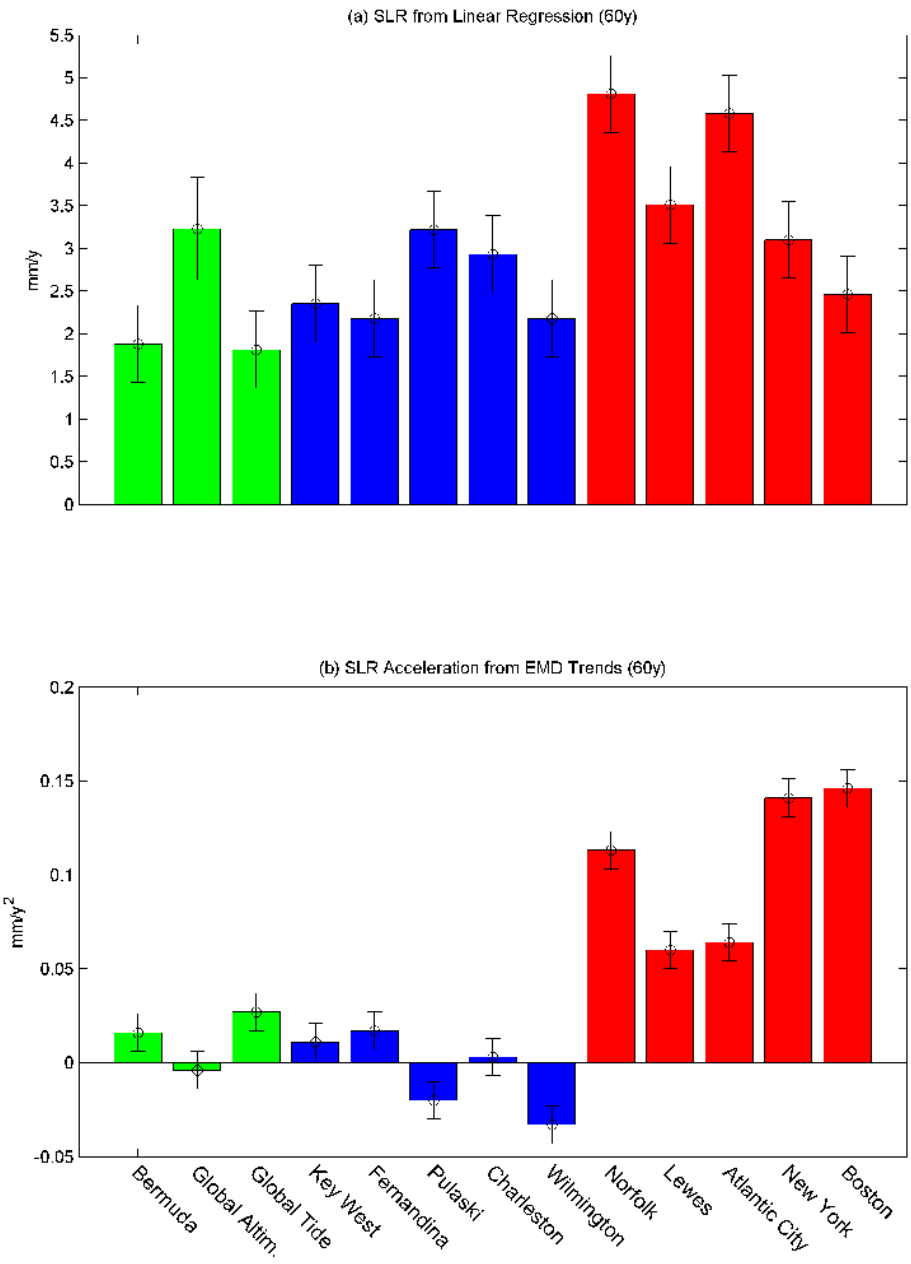

Figure S4. Test of record length impact on SLR trends. (a) Mean SLR from linear regression and (b) acceleration from EMD, as in Fig. 3a-3b, but for only 60 years of tidal records (1952-2012). The Global records end in 2009 and the altimeter record starts in 1993 and is identical to that in Fig. 3.

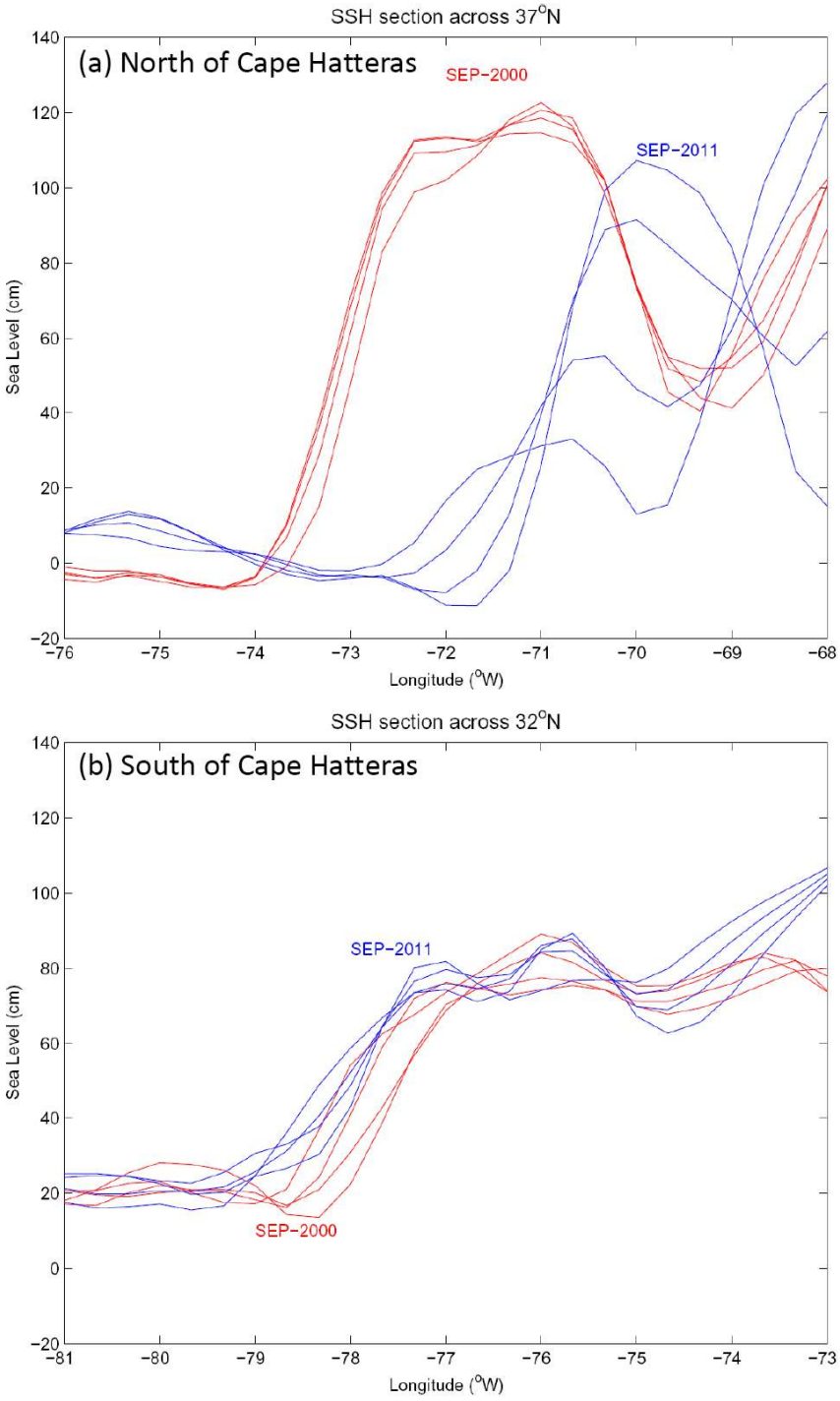

Figure S5. Weekly sea level cross sections from altimeter data (AVISO) during September, 2000 (red lines) and September, 2011 (blue lines). (a) North of Cape Hatteras at 37°N (similar latitude as Norfolk, VA) and (b) South of Cape Hatteras at 32°N (similar latitude as Fort Pulaski, GA).